

Curvilinear Finite Difference Method for Three-Dimensional Potential Problems

P. C. M. LAU

Civil Engineering Department, The University of Western Australia, Nedlands, Australia

Received February 27, 1978; revised November 9, 1978

A numerical solution method for the three dimensional potential problem is presented using finite difference expressions based on curvilinear coordinates and a numerical equation transformation. The computing algorithm is readily programmable. The curvilinear mesh is flexible in discretising the regions near a boundary of general shape. Examples of applications indicate that an irregular mesh can be used and a curved surface requires no special computational treatment.

INTRODUCTION

Many previous finite difference solutions of three dimensional potential problems use a rectangular mesh to discretise the solid. The curved surface is approximated by a planar surface. The normal derivative boundary condition prescribed on the curved surface needs special computational treatment to clarify the ambiguity at a sharp corner. The advantages of relaxing these restrictions are obvious. The problems of discretisation on a curved boundary, the normal derivative boundary condition and the use of a non-rectangular mesh for two dimensional problems are tackled by the Curvilinear Finite Difference Method (1,¹ 2). In this paper the method is extended to the three dimensional case. The Curvilinear Finite Difference Method is based on the equation transformation technique. The governing partial differential equation of the field function is first transformed into local curvilinear α , β and η coordinates before the difference expressions for the partial derivatives are substituted to obtain a system of simultaneous linear equations of the discrete field function. A twenty-seven node curvilinear coordinate system is required to establish the equations for the transformation. The remaining computational procedures are similar to the standard finite difference method. Examples of applications include steady temperature distribution problems in a solid cube and a wedge cut off from a cylinder and the potential problem of a hollow sphere.

¹ The terms A_3 and A_4 of eqt. 8 in ref. 1 should read $A_3 = (T_x^\alpha)^2 + (T_y^\alpha)^2$ and $A_4 = 2(T_x^\alpha T_x^\beta + T_y^\alpha T_y^\beta)$.

BASIC RELATIONSHIPS

To illustrate how the curvilinear difference technique can be applied to the three dimensional potential problem, consider the potential function ψ on a three dimensional region V (Fig. 1) which is required to satisfy the following governing equations:

$$\frac{\partial^2 \psi}{\partial x^2} + \frac{\partial^2 \psi}{\partial y^2} + \frac{\partial^2 \psi}{\partial z^2} = 0 \quad \text{in region } V \quad (1)$$

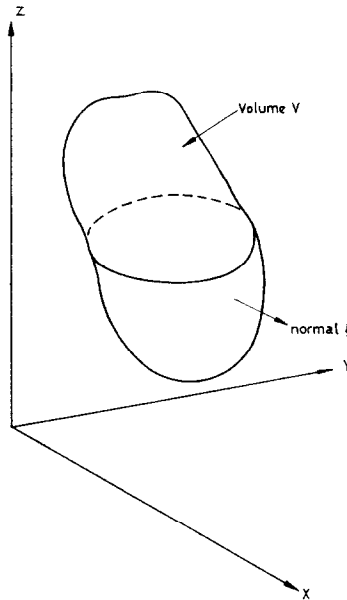


FIG. 1. 3-D solid.

subject to the boundary conditions

$$\psi = \bar{\psi} \text{ on boundary } S_1 \quad \text{and} \quad \frac{\partial \psi}{\partial \eta} = \bar{q} \text{ on boundary } S_2 \quad (2)$$

where $S = S_1 + S_2$ and S denotes the total boundary.

DEFINITIONS OF LOCAL CURVILINEAR α, β, η COORDINATES

Consider the three dimensional region formed by 27 nodes shown in Fig. 2. The mesh is defined by the curvilinear coordinates $\alpha = (0, \pm 1)$, $\beta = (0, \pm 1)$ and $\eta = (0, \pm 1)$.

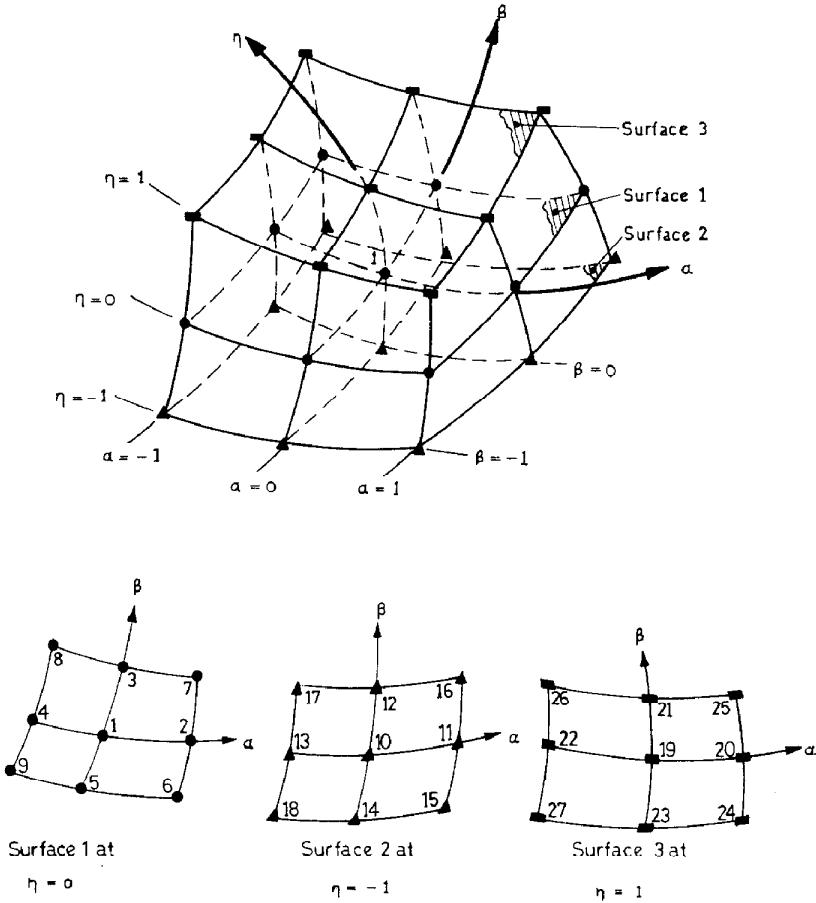


FIG. 2. 3-D curvilinear mesh of 27 node system.

Within this region, the function u is approximated as

$$\begin{aligned}
 u = & a_1 + a_2\alpha + a_3\alpha^2 + a_4\beta + a_5\beta\alpha + a_6\beta\alpha^2 + a_7\beta^2 + a_8\alpha\beta^2 + a_9\beta^2\alpha^2 \\
 & + a_{10}\eta + a_{11}\eta\alpha + a_{12}\eta\alpha^2 + a_{13}\eta\beta + a_{14}\eta\beta\alpha + a_{15}\eta\beta\alpha^2 + a_{16}\eta\beta^2 \\
 & + a_{17}\eta\alpha\beta^2 + a_{18}\eta\beta^2\alpha^2 + a_{19}\eta^2 + a_{20}\eta^2\alpha + a_{21}\eta^2\alpha^2 + a_{22}\eta^2\beta \\
 & + a_{23}\eta^2\beta\alpha + a_{24}\eta^2\beta\alpha^2 + a_{25}\eta^2\beta^2 + a_{26}\eta^2\alpha\beta^2 + a_{27}\eta^2\beta^2\alpha^2
 \end{aligned} \tag{3}$$

where a_1, a_2, \dots, a_{27} are constant coefficients. Equation (3) is more conveniently expressed as

$$u = \phi^T U_p \tag{4}$$

where ϕ is the 27×1 matrix of the interpolation functions given in Appendix 1

and U_p are the 27 nodal values of the unknown in the order $u_1, u_2, u_3, \dots, u_{27}$ i.e.

$$U_p^T = \{u_1 u_2 u_3 \cdots u_{27}\}. \quad (5)$$

Similarly, the coordinates of the 27 nodes can be related to the x, y, z coordinate system using the same interpolation, i.e.

$$\begin{aligned} x &= \phi^T X_p \\ y &= \phi^T Y_p \\ z &= \phi^T Z_p \end{aligned} \quad (6)$$

where X_p, Y_p and Z_p are the x, y and z coordinates of the 27 nodes given as:

$$\begin{aligned} X_p^T &= \{x_1 x_2 x_3 \cdots x_{27}\} \\ Y_p^T &= \{y_1 y_2 y_3 \cdots y_{27}\} \\ Z_p^T &= \{z_1 z_2 z_3 \cdots z_{27}\}. \end{aligned} \quad (7)$$

TRANSFORMATION OF GOVERNING EQUATION INTO CURVILINEAR α, β, η COORDINATES

Before the governing partial differential equation is transformed into the local α, β, η coordinate system, consider the transformation of $\partial u/\partial x, \partial u/\partial y$ and $\partial u/\partial z$ where x, y and z refer to the global coordinate system. The counterpart of $\partial u/\partial x, \partial u/\partial y$ and $\partial u/\partial z$ in the α, β, η coordinate system are $\partial u/\partial \alpha, \partial u/\partial \beta$ and $\partial u/\partial \eta$ respectively. Using the chain rule of the partial differentiation, the relationships between these partial derivatives can be written as

$$\begin{aligned} \frac{\partial u}{\partial x} &= \frac{\partial \alpha}{\partial x} \frac{\partial u}{\partial \alpha} + \frac{\partial \beta}{\partial x} \frac{\partial u}{\partial \beta} + \frac{\partial \eta}{\partial x} \frac{\partial u}{\partial \eta} \\ \frac{\partial u}{\partial y} &= \frac{\partial \alpha}{\partial y} \frac{\partial u}{\partial \alpha} + \frac{\partial \beta}{\partial y} \frac{\partial u}{\partial \beta} + \frac{\partial \eta}{\partial y} \frac{\partial u}{\partial \eta} \\ \frac{\partial u}{\partial z} &= \frac{\partial \alpha}{\partial z} \frac{\partial u}{\partial \alpha} + \frac{\partial \beta}{\partial z} \frac{\partial u}{\partial \beta} + \frac{\partial \eta}{\partial z} \frac{\partial u}{\partial \eta}. \end{aligned} \quad (8)$$

The above equations can be expressed in indicial notation for convenience as

$$U_{,i} = T_i^m U_{,m} \quad (9)$$

where subscript i and m refer to the global x, y, z and local α, β, η coordinate systems respectively, the comma in equation (9) denotes partial differentiation. Similarly the second order partial derivatives $\partial^2/\partial x^2, \partial^2/\partial y^2$ and $\partial^2/\partial z^2$ can be obtained by operating on equation (9) as follows:

Let

$$\begin{aligned}
 V &= U_{,i} \\
 V_{,j} &= (U_{,i})_j = U_{,ij}
 \end{aligned}
 \tag{10}$$

Using equation (9), equation (10) can be written as

$$U_{,ij} = T_j^n (T_i^m U_{,m})_{,n}$$

or

$$U_{,ij} = T_j^n T_{i,n}^m U_{,m} + T_i^m T_j^n U_{,mn} \tag{11}$$

The governing equation of the potential problem given in equation (1) can now be transformed into the local α, β, η coordinate system as

$$\begin{aligned}
 \frac{\partial^2 \psi}{\partial x^2} + \frac{\partial^2 \psi}{\partial y^2} + \frac{\partial^2 \psi}{\partial z^2} &= (T_x^n T_{x,n}^m + T_y^n T_{y,n}^m + T_z^n T_{z,n}^m) \psi_{,m} \\
 &\quad + (T_x^n T_x^m + T_y^n T_y^m + T_z^n T_z^m) \psi_{,mn} \\
 &= 0
 \end{aligned}
 \tag{12}$$

where symmation takes place for the repeated indices. Expanding the right hand side of equation (12) one obtains

$$\begin{aligned}
 \psi_{,xx} + \psi_{,yy} + \psi_{,zz} &= A_1 \psi_{,\alpha} + A_2 \psi_{,\beta} + A_3 \psi_{,\eta} + A_4 \psi_{,\alpha\alpha} + A_5 \psi_{,\beta\beta} \\
 &\quad + A_6 \psi_{,\eta\eta} + A_7 \psi_{,\alpha\beta} + A_8 \psi_{,\beta\eta} + A_9 \psi_{,\eta\alpha}
 \end{aligned}
 \tag{13}$$

where

$$\begin{aligned}
 A_1 &= \sum^{n=\alpha,\beta,\eta} (T_x^n T_{x,n}^\alpha + T_y^n T_{y,n}^\alpha + T_z^n T_{z,n}^\alpha) \\
 A_2 &= \sum^{n=\alpha,\beta,\eta} (T_x^n T_{x,n}^\beta + T_y^n T_{y,n}^\beta + T_z^n T_{z,n}^\beta) \\
 A_3 &= \sum^{n=\alpha,\beta,\eta} (T_x^n T_{x,n}^\eta + T_y^n T_{y,n}^\eta + T_z^n T_{z,n}^\eta) \\
 A_4 &= (T_x^\alpha)^2 + (T_y^\alpha)^2 + (T_z^\alpha)^2 \\
 A_5 &= (T_x^\beta)^2 + (T_y^\beta)^2 + (T_z^\beta)^2 \\
 A_6 &= (T_x^\eta)^2 + (T_y^\eta)^2 + (T_z^\eta)^2 \\
 A_7 &= 2T_x^\alpha T_x^\beta + 2T_y^\alpha T_y^\beta + 2T_z^\alpha T_z^\beta \\
 A_8 &= 2T_x^\beta T_x^\eta + 2T_y^\beta T_y^\eta + 2T_z^\beta T_z^\eta \\
 A_9 &= 2T_x^\eta T_x^\alpha + 2T_y^\eta T_y^\alpha + 2T_z^\eta T_z^\alpha.
 \end{aligned}
 \tag{14}$$

COMPUTATION OF THE COEFFICIENTS T_i^n AND $T_{i,m}^n$

The coefficients T_i^n of node 1 (figure 2) of a 27 node coordinate system can be obtained from the matrix inversion of the Jacobian matrix J as follows:

$$J = \begin{bmatrix} \frac{\partial x}{\partial \alpha} & \frac{\partial y}{\partial \alpha} & \frac{\partial z}{\partial \alpha} \\ \frac{\partial x}{\partial \beta} & \frac{\partial y}{\partial \beta} & \frac{\partial z}{\partial \beta} \\ \frac{\partial x}{\partial \eta} & \frac{\partial y}{\partial \eta} & \frac{\partial z}{\partial \eta} \end{bmatrix}. \quad (15)$$

Using Equation (4)

$$J = \begin{bmatrix} \frac{\partial \phi^T}{\partial \alpha} X_p & \frac{\partial \phi^T}{\partial \alpha} Y_p & \frac{\partial \phi^T}{\partial \alpha} Z_p \\ \frac{\partial \phi^T}{\partial \beta} X_p & \frac{\partial \phi^T}{\partial \beta} Y_p & \frac{\partial \phi^T}{\partial \beta} Z_p \\ \frac{\partial \phi^T}{\partial \eta} X_p & \frac{\partial \phi^T}{\partial \eta} Y_p & \frac{\partial \phi^T}{\partial \eta} Z_p \end{bmatrix} \quad (16)$$

and

$$J^{-1} = \begin{bmatrix} \frac{\partial \alpha}{\partial x} & \frac{\partial \beta}{\partial x} & \frac{\partial \eta}{\partial x} \\ \frac{\partial \alpha}{\partial y} & \frac{\partial \beta}{\partial y} & \frac{\partial \eta}{\partial y} \\ \frac{\partial \alpha}{\partial z} & \frac{\partial \beta}{\partial z} & \frac{\partial \eta}{\partial z} \end{bmatrix}. \quad (17)$$

Hence

$$\begin{bmatrix} T_x^\alpha & T_x^\beta & T_x^\eta \\ T_y^\alpha & T_y^\beta & T_y^\eta \\ T_z^\alpha & T_z^\beta & T_z^\eta \end{bmatrix} = J^{-1}. \quad (18)$$

Carrying out the matrix inversion operation, one obtains

$$\begin{aligned} T_x^\alpha &= \frac{\partial \alpha}{\partial x} = \left(\frac{\partial y}{\partial \beta} \frac{\partial z}{\partial \eta} - \frac{\partial z}{\partial \beta} \frac{\partial y}{\partial \eta} \right) / G \\ T_x^\beta &= \frac{\partial \beta}{\partial x} = \left(\frac{\partial z}{\partial \alpha} \frac{\partial y}{\partial \eta} - \frac{\partial y}{\partial \alpha} \frac{\partial z}{\partial \eta} \right) / G \\ T_x^\eta &= \frac{\partial \eta}{\partial x} = \left(\frac{\partial y}{\partial \alpha} \frac{\partial z}{\partial \beta} - \frac{\partial z}{\partial \alpha} \frac{\partial y}{\partial \beta} \right) / G \\ T_y^\alpha &= \frac{\partial \alpha}{\partial y} = \left(\frac{\partial z}{\partial \beta} \frac{\partial x}{\partial \eta} - \frac{\partial x}{\partial \beta} \frac{\partial z}{\partial \eta} \right) / G \end{aligned}$$

$$\begin{aligned}
 T_y^\beta &= \frac{\partial \beta}{\partial y} = \left(\frac{\partial x}{\partial \alpha} \frac{\partial z}{\partial \eta} - \frac{\partial z}{\partial \alpha} \frac{\partial x}{\partial \eta} \right) / G \\
 T_y^\eta &= \frac{\partial \eta}{\partial y} = \left(\frac{\partial z}{\partial \alpha} \frac{\partial x}{\partial \beta} - \frac{\partial x}{\partial \alpha} \frac{\partial z}{\partial \beta} \right) / G \\
 T_z^\alpha &= \frac{\partial \alpha}{\partial z} = \left(\frac{\partial x}{\partial \beta} \frac{\partial y}{\partial \eta} - \frac{\partial y}{\partial \beta} \frac{\partial x}{\partial \eta} \right) / G \\
 T_z^\beta &= \frac{\partial \beta}{\partial z} = \left(\frac{\partial y}{\partial \alpha} \frac{\partial x}{\partial \eta} - \frac{\partial x}{\partial \alpha} \frac{\partial y}{\partial \eta} \right) / G \\
 T_z^\eta &= \frac{\partial \eta}{\partial z} = \left(\frac{\partial x}{\partial \alpha} \frac{\partial y}{\partial \beta} - \frac{\partial y}{\partial \alpha} \frac{\partial x}{\partial \beta} \right) / G
 \end{aligned} \tag{19}$$

and G is the determinant of the Jacobian matrix J of equation (15).

The second transformation coefficients $T_{i,m}^n$ can be obtained by direct partial differentiating of the coefficients T_i^n of equation (19). Some examples are

$$\begin{aligned}
 T_{x,\alpha}^\alpha &= \frac{\partial}{\partial \alpha} \left(\frac{\partial}{\partial x} \right) \\
 &= \left[\frac{\partial}{\partial \alpha} \left(\frac{\partial y}{\partial \beta} \frac{\partial z}{\partial \eta} - \frac{\partial z}{\partial \beta} \frac{\partial y}{\partial \eta} \right) \cdot G - \left(\frac{\partial y}{\partial \beta} \frac{\partial z}{\partial \eta} - \frac{\partial z}{\partial \beta} \frac{\partial y}{\partial \eta} \right) \frac{\partial G}{\partial \alpha} \right] / G^2 \\
 T_{z,\beta}^\eta &= \frac{\partial}{\partial \beta} \left(\frac{\partial \eta}{\partial z} \right) \\
 &= \left[\frac{\partial}{\partial \beta} \left(\frac{\partial x}{\partial \alpha} \frac{\partial y}{\partial \beta} - \frac{\partial y}{\partial \alpha} \frac{\partial x}{\partial \beta} \right) \cdot G - \left(\frac{\partial x}{\partial \alpha} \frac{\partial y}{\partial \beta} - \frac{\partial y}{\partial \alpha} \frac{\partial x}{\partial \beta} \right) \frac{\partial G}{\partial \beta} \right] / G^2
 \end{aligned} \tag{20}$$

The above expressions indicate that the second order partial derivatives of the coordinates x, y and z are required. These derivatives can be obtained from equation (4).

ALGEBRAIC EXPRESSIONS OF $\psi_{,n}$ AND $\psi_{,nm}$

The local partial derivatives $\partial\psi/\partial\alpha, \partial\psi/\partial\beta, \partial\psi/\partial\eta$ etc. at the centre node 1 can be obtained by substituting $\alpha = \beta = \eta = 0$ into equations (9) and (11). These algebraic expressions are given as

$$\begin{aligned}
 \frac{\partial \psi}{\partial \alpha} &= (\psi_2 - \psi_4) / 2 \\
 \frac{\partial \psi}{\partial \eta} &= (\psi_3 - \psi_5) / 2 \\
 \frac{\partial \psi}{\partial \eta} &= (\psi_{19} - \psi_{10}) / 2
 \end{aligned}$$

$$\begin{aligned}\frac{\partial^2 \psi}{\partial \alpha^2} &= (\psi_2 - 2\psi_1 + \psi_4) \\ \frac{\partial^2 \psi}{\partial \beta^2} &= (\psi_3 - 2\psi_1 + \psi_6) \\ \frac{\partial^2 \psi}{\partial \eta^2} &= (\psi_{19} - 2\psi_1 + \psi_{10}) \\ \frac{\partial^2 \psi}{\partial \alpha \partial \beta} &= (\psi_7 - \psi_8 + \psi_9 - \psi_6)/4 \\ \frac{\partial^2 \psi}{\partial \beta \partial \eta} &= (\psi_{20} - \psi_{22} + \psi_{13} - \psi_{11})/4 \\ \frac{\partial^2 \psi}{\partial \eta \partial \alpha} &= (\psi_{21} - \psi_{23} + \psi_{14} - \psi_{12})/4\end{aligned}$$

Similarly, the algebraic expressions of the partial derivatives of x , y and z with respect to α , β and η defined in equation (16) can be obtained from equation (21) after replacing ψ by the appropriate x , y or z .

TRANSFORMED GOVERNING EQUATION

The algebraic expression of equation (1) can now be obtained by substituting equations (14), (19) and (20) into (13) giving

$$R_1\psi_1 + R_2\psi_2 \cdots R_{27}\psi_{27} = 0 \quad (22)$$

where the non-zero coefficients R_i are

$$\begin{aligned}R_1 &= -2(A_4 + A_5 + A_6) \\ R_2 &= A_4 + A_1/2 \\ R_3 &= A_4 + A_1/2 \\ R_4 &= A_5 + A_2/2 \\ R_5 &= A_5 - A_2/2 \\ R_6 &= -A_7/4 \\ R_7 &= A_7/4 \\ R_8 &= -A_7/4 \\ R_9 &= A_7/4 \\ R_{10} &= A_6 - A_3/2 \\ R_{11} &= -A_9/4 \\ R_{12} &= -A_8/4 \\ R_{13} &= A_9/4\end{aligned}$$

$$\begin{aligned}
 R_{14} &= A_8/4 \\
 R_{19} &= A_6 + A_3/2 \\
 R_{20} &= A_9/4 \\
 R_{21} &= A_8/4 \\
 R_{22} &= -A_9/4 \\
 R_{23} &= -A_8/4
 \end{aligned}$$

The coefficients R_{15} , R_{16} , R_{17} , R_{18} , R_{24} , R_{25} , R_{26} and R_{27} are all equal to zero indicating that only 19 unknowns ψ are involved in equation 22. The 27 node system can be reduced to a 19 node system without losing any terms of the approximate u function in equation 3 as the computation of T_i^n and $T_{i,m}^n$ does not require the x , y and z coordinates of nodes 15, 16, 17, 18, 24, 25, 26 and 27.

BOUNDARY CONDITIONS

On the boundary S_1 , where $\psi = \bar{\psi}$, the discrete value of $\bar{\psi}_i$ at the node i is $\bar{\psi}$. On the boundary S_2 where the normal derivative is zero, the discrete value ψ_i at the node is to be computed. The equation (26) must be applied to this node i . The local region overlaps both inside and outside part of region V and generates outside node j .

The normal derivative condition is used to compute ψ_j at node j as in the case of the standard finite difference method. The present curvilinear finite difference can easily satisfy this condition on the curved boundary. This is done by choosing any one of the α , β , η lines to coincide with the normal ξ (figure 3). The outside node j is related to the inside node k as $\psi_j = \psi_k + \bar{q} * a$. The coordinates x_j , y_j and z_j of node j are required for the setting up of the local curvilinear coordinate system but ψ_j is not included in the system of simultaneous linear equations.

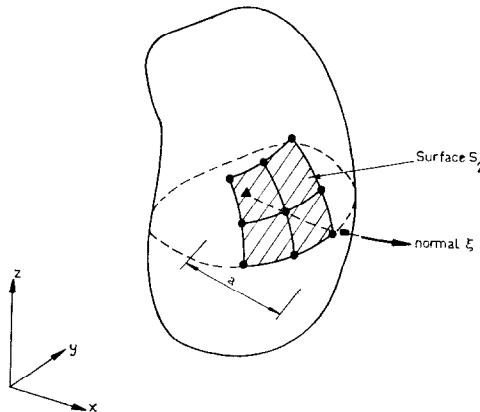


FIG. 3. Normal derivative boundary condition on curved surface.

SOLUTION OF THE GLOBAL EQUATION OF DISCRETE ψ_i

Applying equation (26) to every one of the interior nodes and the nodes on the boundary S_2 of the region, a system of simultaneous linear equations governing the discrete values of the potential function ψ can be obtained. The solution of this equation can be by either direct or iterative solution methods. The direct method usually employs the more general Gaussian elimination method taking advantage of the banded form of the coefficients of the unsymmetric matrix. The iterative methods such as Gauss-Seidel or Successive Over Relaxation methods require fewer arithmetic operations and less computer storage as there are at most 19 non-zero coefficients in any row of the matrix.

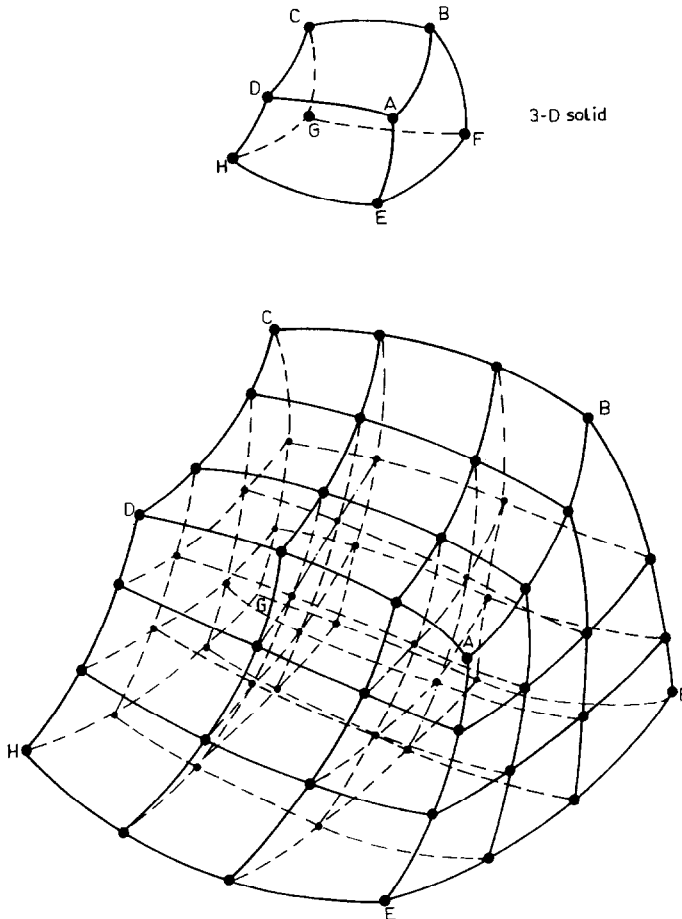


FIG. 4. Typical 3-D curvilinear mesh.

COMPUTATIONAL PROCEDURE

The computational procedure of the curvilinear finite difference method is similar to the standard finite difference method except that it requires the additional information of the nodal x, y and z coordinates and the equation transformation. The steps are summarised as:

- (a) Discretise the region V into curvilinear meshes (see figure 4).
- (b) Assign nodal numbers and x, y, z coordinates to the nodes and form local α, β, η coordinate system.
- (c) Set up the global equation of the discrete ψ_i by applying equation (26) to all interior nodes in region V and the nodes on the boundary S_2 .
- (d) Inject the boundary condition of the boundary node (i.e. $\psi_i = 0$ or $\psi_j = \psi_k + \bar{q} * a$ by modifying the equations obtained in step (c).
- (e) Solve the modified equations in step (d) to obtain the discrete potentials ψ_i .

EXAMPLES OF APPLICATIONS

Regular and irregular meshes, particularly a graded mesh, are used to analyse three field problems by the Curvilinear Finite Difference Method. The numerical accuracy of the method is tested by varying the size of the mesh and increasing the

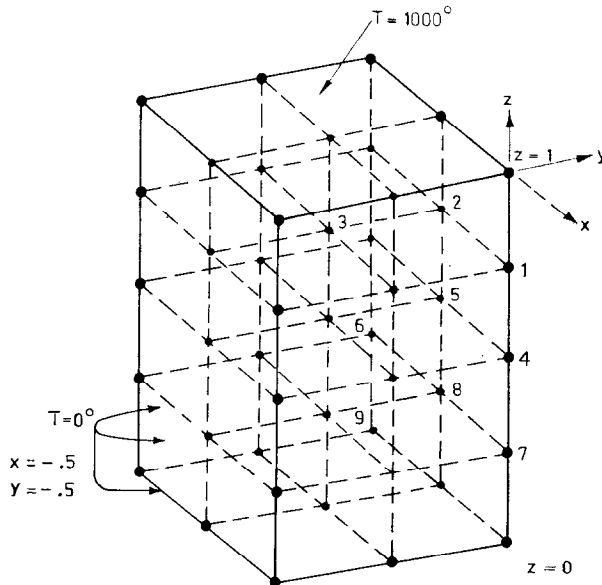


FIG. 5. Mesh discretisation of a unit cube ($\frac{1}{4}$ of solid shown).

number of the discrete field unknowns. The computer program written for the 3-*D* analysis is modified from the 2-*D* computer program FIELD reported in reference [2]. The minor changes are the input data information and the program SUBROUTINE TMAT and COEF. The data information for the present analysis requires the coordinates x , y and z of the nodes, the nodal numbers of the nodes forming the curvilinear meshes and the boundary conditions. All the data are generated by a separate program. The data generation is possible as the curvilinear mesh of different sizes follow the same pattern. The system of simultaneous linear equations is solved by an iterative Gauss-Seidel method to reduce computer storage requirement.

TABLE 1
Comparison of Temperature Distribution of Unit Cube (Figure 5)

Mesh grade (no. of mesh, no. of unknowns)	Temperatures at nodes									Remarks
	1	2	3	4	5	6	7	8	9	
coarse $1 \times 1 \times 2$ mesh 1 unknown	—	—	—	167	—	—	—	—	—	<i>C.F.D.</i> regular grid
medium $2 \times 2 \times 4$ 12 unknowns	435	361	303	163	127	98	54	40	30	<i>C.F.D.</i> regular grid
fine $4 \times 4 \times 8$ 70 unknowns	452	370	308	169	127	96	57	31	23	<i>C.F.D.</i> regular grid
—	454	371	307	167	123	92	52	37	27	Finite Element method ref 3, 4
—	458	373	307	167	123	91	51	37	26	Finite Difference Method ref 3, 4
—	458	—	—	167	—	—	51	—	—	Analytical solution by series solution

TEMPERATURE DISTRIBUTION OF UNIT CUBE

The steady state temperature distribution of a unit cube (figure 5) subject to zero temperature on five faces and a constant temperature of 1000°C on the top face is investigated by the C.F.D. method using various mesh discretisations. The comparison of the present results with the finite element and the standard finite difference results are summarised in the table 1. The effect of the irregular mesh on the numerical results, particularly the graded mesh discretisation in which more meshes are used for the

TABLE 2
Comparison of Temperature T and $\partial T/\partial z$ at Nodes (Figure 5)

Mesh grade (no. of mesh, no. of unknowns)	Vertical distance, z	Temperature at nodes		Relative dimension of vertical mesh
		T	$\partial T/\partial z$	
medium $2 \times 2 \times 4$ mesh 12 unknowns	0.85	606	2079	0.15/0.2/0.275/ 0.375 irregular
		650 ^a	2127 ^a	
	0.65	272	1099	
	0.375	311 ^a	1240 ^a	
		84	419	
		95 ^a	444 ^a	
medium $2 \times 2 \times 4$ mesh 12 unknowns	0.8	512	1937	0.2/0.2/0.3/0.3 irregular
		548 ^a	1919 ^a	
	0.6	225	896	
		254 ^a	1047 ^a	
	0.3	645	375	
		709 ^a	337 ^a	
fine $4 \times 4 \times 8$ mesh 70 unknowns	0.9	750	2330	0.1/0.1/0.1/ 0.1625/.1625/ 0.125/0.125/0.125 irregular
		760 ^a	2290 ^a	
	0.8	534	1929	
		548 ^a	1919 ^a	
	0.125	29	182	
		22 ^a	194 ^a	
very fine $5 \times 5 \times 10$ mesh 135 unknowns	0.9	755	2285	vertical mesh at 0.1 unit distance apart
		760 ^a	2290 ^a	
	0.8	543	1897	
		548 ^a	1919 ^a	
	0.6	254	1038	
		254 ^a	1047 ^a	

^a Meshes are kept uniform in x, y plane but varies in the z direction. Analytical results are marked with asterisks.

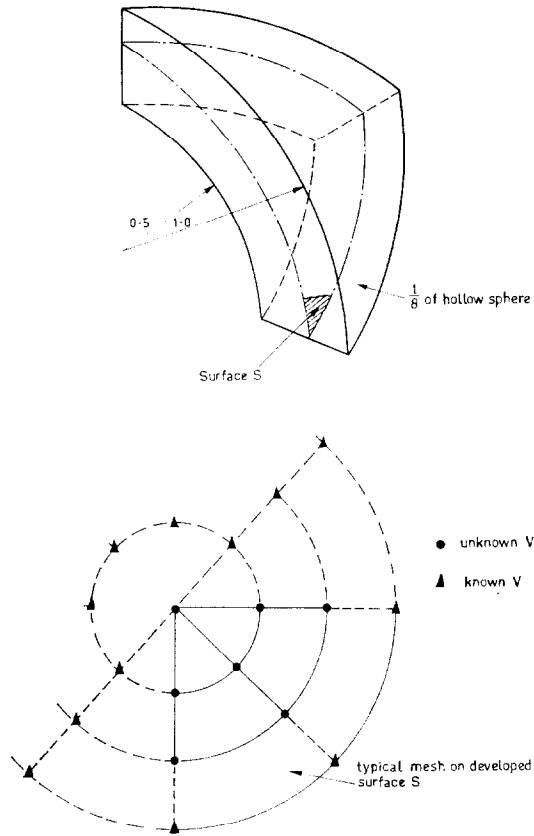


FIG. 6. Hollow sphere.

region where rapid changes of the temperature are expected, are also studied. The comparison of the results obtained from the C.F.D. method and the analytical method are shown in table 2. In all the analyses the computed temperature and the rate of change of the temperature are found in good agreement with the analytical solution.

ELECTROSTATIC POTENTIAL OF A HOLLOW SPHERE

The outer sphere (radius = 1) is held at constant potential V_0 and the inner sphere (radius = 0.5) is held at zero potential (figure 6). The explicit finite difference expressions of coefficients can be obtained after transforming the governing potential equation 1 into a spherical coordinate system. The table 3 summarises the comparison of the finite difference coefficients of the C.F.D. and the exact methods. Various mesh sizes are studied and both methods are found in good agreement except the very coarse meshes (Figure 7). The potentials of the sphere shown in table 4 are very close

TABLE 3

Comparison of the Finite Difference Coefficients R_i Computed by C.F.D. and Exact Methods

Finite difference coefficients R_i of eq. (26) by C.F.D.	Different meshes (figure 6)						
	$\Delta r = .1$	$\Delta r = .1$	$\Delta r = .1$	$\Delta r = .1$	$\Delta r = .5$	$\Delta r = .5$	$\Delta r = .5$
	$\Delta\theta = 5^\circ$ $\Delta\phi = 5^\circ$	$\Delta\theta = 10^\circ$ $\Delta\phi = 10^\circ$	$\Delta\theta = 50^\circ$ $\Delta\phi = 50^\circ$	$\Delta\theta = 100^\circ$ $\Delta\phi = 100^\circ$	$\Delta\theta = 10^\circ$ $\Delta\phi = 10^\circ$	$\Delta\theta = 50^\circ$ $\Delta\phi = 50^\circ$	$\Delta\theta = 100^\circ$ $\Delta\phi = 100^\circ$
R_1	-726.6 -725.3 ^a	-332.7 -331.1 ^a	-206.8 -205.3 ^a	-204.1 -201.3 ^a	-140.7 -139.3 ^a	-14.8 -13.3 ^a	-12.1 -9.3 ^a
R_2, R_5 R_{10}, R_{19}	110.0 110.0 ^a	110.0 110.0 ^a	110.0 110.0 ^a	110.0 110.0 ^a	6.00 6.00 ^a	6.00 6.00 ^a	6.0 6.0 ^a
R_3	131.7 131.3 ^a	33.2 32.8 ^a	1.7 1.3 ^a	1.0 0.3 ^a	33.2 32.8 ^a	1.7 1.3 ^a	1.0 0.3 ^a
R_4	89.9 90.0 ^a	89.9 90.0 ^a	89.9 90.0 ^a	89.9 90.0 ^a	1.9 2.0 ^a	1.9 2.0 ^a	1.9 2.0 ^a

^a (a) The coordinates x, y, z for computing the coefficients R_i are derived from the r, θ and ϕ of the spherical coordinates. (b) The remaining coefficients R_i not shown are all equal to zero.

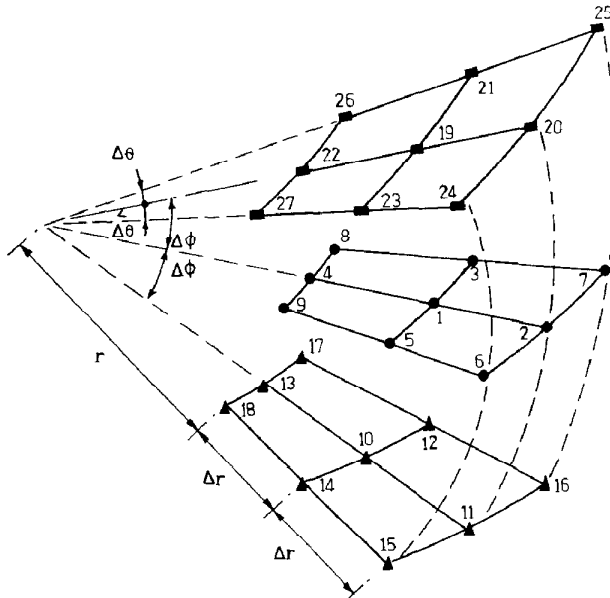


FIG. 7. Mesh generated by spherical coordinates for comparison of exact and numerical transformations.

TABLE 4

Comparison of Electrostatic Potentials of a Hollow Space Computed by C.F.D. and Exact Methods

Mesh	no. of unknowns	node	coordinates of node			electrostatic potential V of node		Remarks
			x	y	z	$V(xV_0)$	$\frac{\partial V}{\partial z}(xV_0)$	
coarse 21 unknowns	A		.315				1.962	regular mesh
			.315			.428		
			.4419			.400 ^a	—	
	B		0				1.225	
			0			.873		
			.875			.857 ^a	—	
	C		.4375				.866	
			.4375			.872		
			.6187			.857 ^a	—	
medium 39 unknowns	A		.2706				1.356	regular mesh
			.4687			.411		
			.3125			.400 ^a	—	
	B		0				1.287	
			0			.863		
			.875			.857 ^a	—	
	C		.3789				.643	
			.6562			.864		
			.4375			.857 ^a	—	
medium 49 unknowns	A		.2813				2.419	regular mesh
			.2812			.241		
			.3977			.222 ^a	—	
	B		0				1.021	
			0			.936		
			.9325			.928 ^a	—	
	C		.4663				.722	
			.4662			.936		
			.6594			.928 ^a	—	

Table continued

TABLE IV (continued)

Comparison of Electrostatic Potentials of a Hollow Space Computed by C.F.D. and Exact Methods

Mesh	no. of unknowns	node	coordinates of node		electrostatic potential V of node		Remarks
			x	y	$V(xV_0)$	$\frac{\partial V}{\partial z}(xV_0)$	
fine 91 unknowns	A		.2436			1.646	regular mesh
			.4219		.230		
			.2813		.222 ^a	—	
	B		0			1.091	
			0		.937		
			.9375		.933 ^a	—	
	C		.4059			.546	
			.7031		.937		
			.4688		.933 ^a	—	
fine 91 unknowns	A		.2436			1.659	irregular mesh
			.4219		.232		
			.2813		.222 ^a	—	
	B		0			1.043	
			0		.951		
			.95		.947 ^a	—	
	C		.4114			.521	
			.7125		.950		
			.4750		.947 ^a	—	

^a Potential V calculated by exact method.

to the analytical solution. This application also shows that the curved surface of the sphere is well approximated by the curvilinear coordinates α , β and η without introducing sharp corners into the discretisation as in the case of using the 4 nodes or 8 nodes solid finite element (3).

Temperature distribution of a wedge

The figure 8 shows a wedge cut off from a right cylinder. The two vertical and the bottom faces are held at zero temperature. The top face is held at 1000° temperature. The curved face is insulated and a zero normal derivative is prescribed. Three mesh discretisations are used to analyse the temperature distribution. The results of temperature and $\partial T/\partial z$ are shown in table 5. This example shows that the normal derivative on a curved surface can be accurately prescribed. The degeneration of the

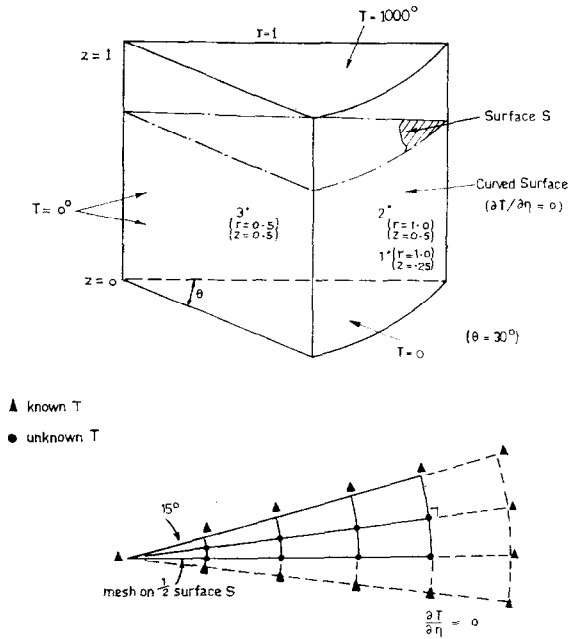


FIG. 8. Wedge cut off from right cylinder.

TABLE 5
Temperature T and $\partial T/\partial z$ of a Wedge (Figure 8)

Mesh (no. of meshes, no. of unknowns)	Temperature T at node			$\partial T/\partial z$ at node			remarks
	1	2	3	1	2	3	
medium $2 \times 4 \times 8$ meshes 56 unknowns	8.41	47.2	7.91	68.78	351.3	89.31	regular mesh vertical division: $4 \times 0.25 = 1$
fine $2 \times 8 \times 8$ meshes 112 unknowns	7.54	43.9	8.07	63.19	337.3	90.00	regular mesh vertical division: $8 \times 0.125 = 1$
fine $2 \times 8 \times 8$ meshes 112 unknowns	7.37	42.9	7.86	61.76	357.3	97.15	graded mesh vertical division: $4 \times 0.165 +$ $2 \times 0.15 + 2 \times 0.1$ $= 1$

mesh from 27 nodes to 21 nodes occurs near the corner region where the two vertical planar surfaces meet.

DISCUSSION AND CONCLUSION

The proposed Curvilinear Finite Difference method attempts to put the finite difference ideas into a more programmable and flexible structure so that the geometric generality of the finite element method is approached. The examples of applications illustrate that (a) a curved surface presents no special problem to the mesh discretisation, (b) the normal derivative on a curved surface is approximated by a central difference expression without any equation transformation and (c) an irregular mesh can be applied to calculate the discrete potential at a specific point with reduction of the computational effort. Table 2 indicates that the temperature at the point with the coordinates ($x = y = 0$, and $z = 0.8$) can be computed with sufficient accuracy by using fewer unknown discrete potentials. The temperature T obtained by the irregular meshes with 12 and 7° unknowns are 512° and 534° respectively. These results compare very favourably with the regular mesh with 135 unknowns case in which T is 543°. The analytical solution for T is 548°.

Unlike the previous Chu's machine transformation (6) using regular hexagonal mesh, the interpolation function approach of the present C.F.D. is also applicable to non-orthogonal curvilinear coordinate system and is flexible to generate a mesh to suit the geometry of the solid particularly the region near the boundary.

The C.F.D. method requires no numerical integration nor the subsequent element assembling procedure of the variational based finite element (3) and the more recent integral equation based methods (5). A direct comparison of the computer time of different methods using the same machine is beyond the scope of this paper. However, the author believes that the Curvilinear Finite Difference method requires less computation effort than the finite element method (3) with explicit and symmetric element matrix. A summary of the comparison of the arithmetic operations of both methods to set up 27 equations are summarised as follows:

	Total number of arithmetic (+ or -) operations	Total number of arithmetic (x or ÷) operations
Finite Element Method (Based on assembling 8 brick elements. Each element is obtained from assembling five tetrahedrons. Only the upper triangle of the matrix is formed, ref. [3])	18400	28480
Present C.F.D. method	10692	9360

The C.F.D. method also requires less computer storage than the F.E method as it only keeps the non-zero coefficients and is independent of the band width if an iterative simultaneous linear equation solution method is used. The computing time of the example on a C.D.C. CYBER 72 machine ranges from 5 to 30 seconds depending the number of discrete potentials.

APPENDIX 1

Interpolation functions ϕ for u approximation (equation (4)) are given as

$$\phi_1^T = \left[\begin{array}{ccc} (1 - \eta^2) \phi_1^T & -\frac{1}{2}(\eta - \eta^2) \phi_1^T & \frac{1}{2}(\eta + \eta^2) \phi_1^T \\ \underset{1 \times 27}{} & \underset{1 \times 9}{} & \underset{1 \times 9}{} \end{array} \right]$$

where

$$\phi_1 = \begin{bmatrix} (1 - \alpha^2 - \beta^2 + \alpha^2\beta^2) \\ (\alpha - \alpha\beta^2 + \alpha^2 - \alpha^2\beta^2)/2 \\ (\beta - \alpha^2\beta + \beta^2 - \alpha^2\beta^2)/2 \\ (-\alpha + \alpha\beta^2 + \alpha^2 - \alpha^2\beta^2)/2 \\ (-\beta + \alpha^2\beta + \beta^2 - \alpha^2\beta^2)/2 \\ (-\alpha\beta - \alpha^2\beta + \alpha\beta^2 + \alpha^2\beta^2)/4 \\ (\alpha\beta + \alpha^2\beta + \alpha\beta^2 + \alpha^2\beta^2)/4 \\ (-\alpha\beta + \alpha^2\beta - \alpha\beta^2 + \alpha^2\beta^2)/4 \\ (\alpha\beta - \alpha^2\beta - \alpha\beta^2 + \alpha^2\beta^2)/4 \end{bmatrix}_{9 \times 1}$$

REFERENCES

1. P. C. M. LAU, *Appl. Math. Modelling* **1** (September, 1977).
2. P. C. M. LAU, "Curvilinear Finite Difference Method of Potential Problems," CE Report, December, 1977, Civil Engineering Department, University of Western Australia.
3. O. C. ZIENKIEWICZ, A. D. BAHRANI, AND P. L. ARLETT, *Engineer* (October 1967), 547-550.
4. D. M. DE ALLEN AND S. C. R. DENNIS, *Quart. J. Mech. Appl. Math.* **4** (Part 2), (1951).
5. G. JENG AND A. WEXLER, *Int. J. Num. Methods Eng.* **14** (1977), 1455-1471.
6. W. H. CHU, *J. Computational Phys.* **8** (1971), 392-408.